

# Three-dimensional structure of an AMPA receptor without associated stargazin/TARP proteins

Terunaga Nakagawa<sup>1,a,\*</sup>, Yifan Cheng<sup>2</sup>, Morgan Sheng<sup>1,\*</sup> and Thomas Walz<sup>2,\*</sup>

<sup>1</sup>The Picower Center for Learning and Memory, RIKEN-MIT Neuroscience Research Center, Howard Hughes Medical Institute, Massachusetts Institute of Technology, 77 Massachusetts Avenue, Cambridge, MA 02139, USA

<sup>2</sup>Department of Cell Biology, Harvard Medical School, 240 Longwood Avenue, Boston, MA 02115, USA

\*Corresponding authors

e-mail: nakagawa@chem.ucsd.edu; msheng@mit.edu; twalz@hms.harvard.edu

## Abstract

Most excitatory synaptic transmissions in the central nervous system are mediated by the neurotransmitter glutamate. Binding of glutamate released from the presynaptic membrane causes glutamate receptors in the postsynaptic membrane to open, which results in a transient depolarization of the postsynaptic membrane. The AMPA ( $\alpha$ -amino-3-hydroxy-5-methyl-4-isoxazole propionic acid) subtype of glutamate receptors is responsible for the majority of excitatory postsynaptic currents and is thought to play a central role in synaptic plasticity. Because modulation of glutamate receptors is believed to be involved in the basic mechanism underlying information storage in the brain, the molecular architecture of native AMPA receptors (AMPA-Rs) is of great interest. Previously, we have shown that AMPA-Rs purified from the brain are tightly associated with members of the stargazin/TARP (transmembrane AMPA receptor regulatory protein) family of membrane proteins [Nakagawa et al., *Nature* 433 (2005), pp. 545–549]. Here, we present a three-dimensional (3D) density map of the hetero-tetrameric AMPA-R without associated stargazin/TARP proteins as determined by cryo-negative stain single-particle electron microscopy. In the absence of stargazin/TARP proteins, the density representing the transmembrane region of the AMPA-R particles is substantially smaller, corroborating our previous analysis that was based solely on projection images.

**Keywords:** AMPA receptor; glutamate receptor; ligand-gated ion channel; membrane protein; stargazin; synapse; synaptic transmission; TARP.

## Introduction

Synapses are specialized structures through which neurons communicate with each other, allowing them to form

neural circuits. Because signals are transmitted between neurons through the synapses, modulation of synaptic transmission is believed to be involved in information processing in the brain, such as seen in learning and memory. In the central nervous system, most excitatory synaptic transmission is mediated by the neurotransmitter glutamate. Glutamate released from the presynaptic membrane activates glutamate receptors, ligand-gated ion channels, in the postsynaptic membrane. Much is known about the electrophysiological properties and trafficking of glutamate receptors, and studies of genetically engineered animals have substantially advanced our understanding of glutamate-mediated synaptic transmission. In contrast, our knowledge of the molecular architecture of glutamate receptor complexes is still very limited.

Based on their distinct pharmacological properties, ionotropic glutamate receptors have been classified into three groups: NMDA (*N*-methyl-D-aspartic acid), AMPA ( $\alpha$ -amino-3-hydroxy-5-methyl-4-isoxazole propionic acid) and kainate receptors (Dingledine et al., 1999). AMPA-Rs are responsible for the majority of excitatory postsynaptic currents in the central nervous system, and they play a critical role in synaptic plasticity (Malinow and Malenka, 2002). The rat genome contains four genes encoding AMPA-R subunits, known as GluR1–4 or GluRA–D (Hollmann et al., 1989; Keinanen et al., 1990; Nakanishi et al., 1990). The four GluR subunits are highly homologous in amino acid sequence, and they share a common domain organization and membrane topology (Figure 1A). On the extracellular side, AMPA-R subunits consist of an N-terminal domain (NTD; also known as amino-terminal domain, ATD) and a ligand-binding domain (LBD). The ligand-binding domain is interrupted in polypeptide sequence by the transmembrane domain (TMD), which includes the ion channel core. The TMD consists of three membrane-spanning segments, M1, M3, and M4, and the M2 ‘re-entrant loop’. The intracellular C-terminal tails of AMPA-R subunits are short compared to the extracellular domains, but they are important for correct trafficking of the receptor. AMPA-R subunits have been proposed to assemble into a hetero-tetramer (Wentholt et al., 1996; Rosenmund et al., 1998), and structural information suggests that they have a dimer-of-dimers organization (Gouaux, 2004; Tichelaar et al., 2004; Figure 1B).

The protocol we used to isolate native AMPA-Rs from rat brain led to the co-purification of all members of the stargazin/TARP family (Figure 1B), namely  $\gamma$ -2 (also known as stargazin, 36 kDa),  $\gamma$ -3 (36 kDa),  $\gamma$ -4 (37 kDa), and  $\gamma$ -8 (43 kDa) (Nakagawa et al., 2005). A similar result was obtained when native AMPA-Rs were purified using an introduced affinity tag, but the structural integrity of receptor complexes purified with this approach has not been established (Vandenberghe et al., 2005b). Stargazin

<sup>a</sup>Present address: Department of Chemistry and Biochemistry, University of California, San Diego, 9500 Gilman Drive, La Jolla, CA 92093-0378, USA

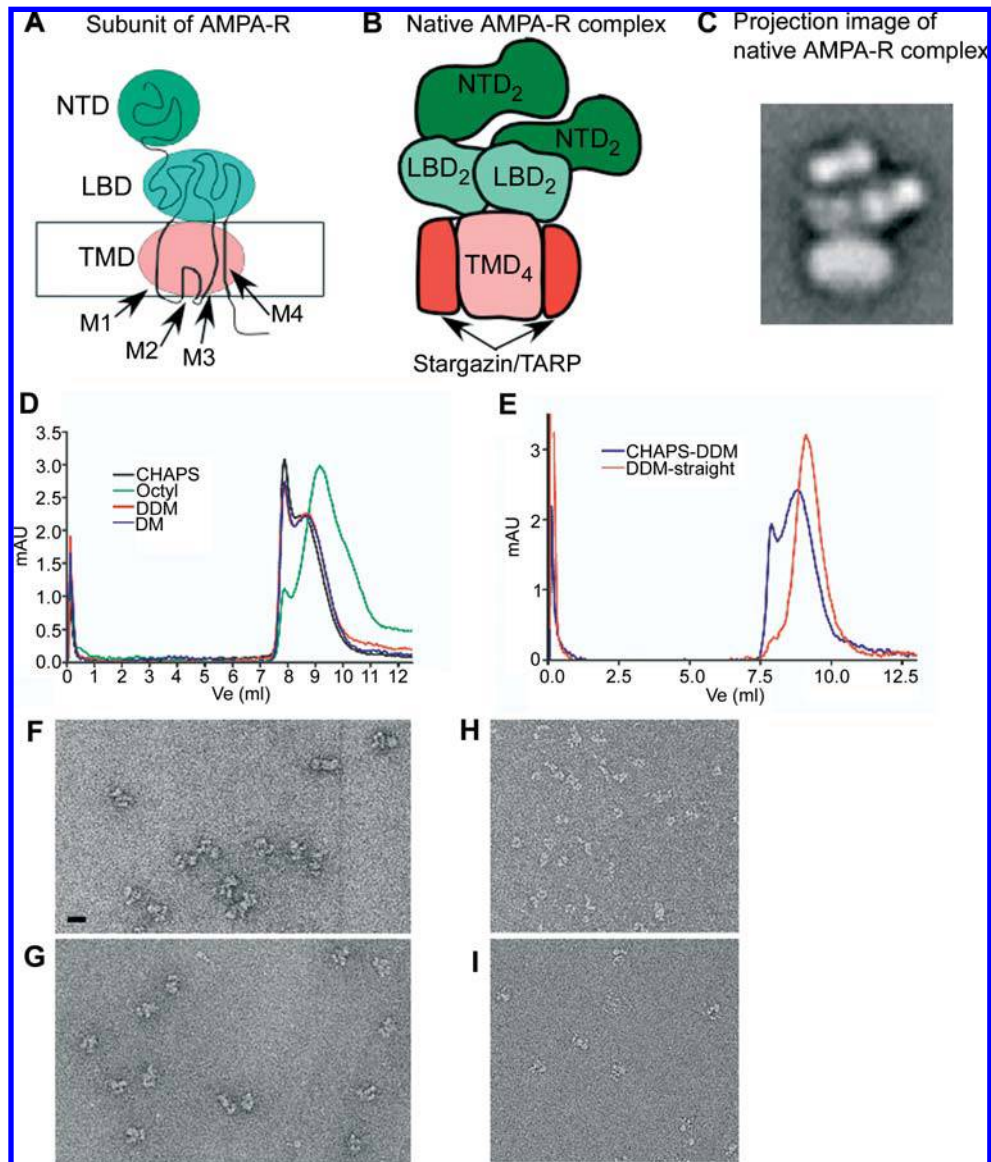


**Figure 1** Molecular architecture of the native AMPA-R complex and its stability in different detergents. (A) Cartoon showing the domain structure of AMPA-R subunits. NTD, N-terminal domain; LBD, ligand-binding domain; and TMD, transmembrane domain. The box represents the lipid bilayer. M1–4 indicate the sub-domains within the TMD. (B) Cartoon depicting a native AMPA-R complex consisting of the hetero-tetrameric AMPA-R and associated stargazin/TARP proteins. (C) Representative class average of a negatively stained native AMPA-R complex in type I conformation. (D) Elution profiles of native AMPA-R complexes that were solubilized from the membrane with CHAPS and further treated with DDM, DM and OG. The original native AMPA-R complex purified in CHAPS eluted slightly earlier than those treated with DM or DDM. AMPA-Rs treated with OG eluted significantly later than those exposed to the other detergents. The peak elution volume ( $V_e$ ) was 8.58 ml for CHAPS, 8.68 ml for DDM, 8.63 ml for DM, and 9.16 ml for OG. (E) Effect of the detergent used to solubilize the membranes on the peak elution volume of purified AMPA-Rs. Native AMPA-R complex that was solubilized with CHAPS and further treated with DDM eluted earlier ( $V_e=8.81$  ml) than the one that was immediately solubilized with DDM ( $V_e=9.11$  ml). (F–I) Images of negatively stained AMPA-R complexes treated with different detergents. (F) AMPA-Rs purified in CHAPS; (G) AMPA-Rs purified in CHAPS and treated with DDM; (H) AMPA-Rs purified in CHAPS and treated with OG; and (I) AMPA-Rs purified from synaptosome-enriched membranes that were directly solubilized with DDM. Scale bar: 16 nm.

was initially identified as a product of the gene that is mutated in the stargazer mutant mouse (Letts et al., 1998). Stargazin/TARP proteins have four membrane-spanning segments and are structurally related to claudins and the  $\gamma$ -subunit of the skeletal muscle voltage-gated calcium channel (Chen et al., 2000; Tomita et al., 2003). Stargazin/TARP proteins play a critical role in the surface expression and synaptic targeting of the AMPA-R in cerebellar granule cells (Chen et al., 2000). The prevailing model holds that the interaction of star-

gazin/TARP proteins with AMPA-Rs is essential for the initial surface expression of the complex, while further translocation of the complex from the extrasynaptic space to the synaptic region is mediated by the interaction of the C-terminus of the stargazin/TARP protein with the PDZ domain of the synaptic scaffold protein PSD-95 (Chen et al., 2000).

Our recent single-particle electron microscopy (EM) study provided direct evidence for the association of stargazin/TARP proteins with AMPA-Rs. Images of puri-

fied AMPA-Rs incubated with Fab fragments specific for the cytoplasmic C-terminus of stargazin/TARP proteins showed that the Fabs localized to the transmembrane region of the native AMPA-R complex (Nakagawa et al., 2005). However, only projection images of the negatively stained particles were examined in these immunolabeling experiments. To confirm that proteins of the stargazin/TARP family indeed contribute to the transmembrane region of native AMPA-R complexes, we performed a 3D structural analysis. Here, we now report the 3D structure of an AMPA-R without associated stargazin/TARP proteins, as determined by cryo-negative stain single-particle EM. We compare this structure to that of the previously determined native AMPA-R complex containing associated stargazin/TARP proteins.

## Results

### Stability of the native AMPA receptor complex in different detergents

To purify native AMPA-R complexes, synaptosome-enriched membranes isolated from rat brain extract were solubilized with CHAPS, and the complexes purified by immunoaffinity chromatography. As reported before, members of the stargazin/TARP family of integral membrane proteins were tightly associated with AMPA-Rs purified in this way (Nakagawa et al., 2005). Accordingly, in images of negatively stained AMPA-Rs isolated in CHAPS, the transmembrane domain of the complex is represented by a large density (Figure 1C, F).

To characterize the structure of the core AMPA-R, we had to establish a purification protocol that stripped off the co-purifying stargazin/TARP proteins without destroying the structural integrity of the AMPA-Rs. To this end we exposed native AMPA-R complexes purified in CHAPS to the slightly stronger detergents dodecyl maltoside (DDM), decyl maltoside (DM), and octyl glucoside (OG). Exposure of the AMPA-R particles to OG resulted in a loss of structural integrity as determined by negative stain EM (Figure 1H). This observation was further supported by the finding that OG-treated particles eluted significantly more slowly from gel filtration columns compared to untreated particles (Figure 1D). Treatment of native AMPA-R complexes with DDM and DM compromised the structural integrity of the particles much less, and the particles consistently eluted at an elution volume similar to that for untreated particles (Figure 1D). As reported before, DDM and DM treatment can dissociate stargazin/TARP proteins from AMPA-Rs (Nakagawa et al., 2005). Consistently, careful observation of the gel filtration chromatography traces revealed that AMPA-R particles in DDM and DM eluted slightly more slowly than particles prepared in CHAPS (Figure 1D).

Gel filtration chromatography and negative stain EM analysis identified DDM as the most suitable detergent to isolate structurally intact AMPA-Rs without associated stargazin/TARP proteins. We therefore attempted to simplify the purification protocol and to directly solubilize the synaptosome-enriched membranes with DDM. However, AMPA-Rs solubilized from membranes directly with DDM eluted at a substantially different elution volume from the gel filtration column than AMPA-Rs solubilized with

CHAPS and subsequently treated with DDM (Figure 1E). Furthermore, a large fraction of the particles appeared to be damaged when visualized by negative stain EM (Figure 1I). These results suggest that the choice of detergent used to solubilize the membranes has a significant effect on the preservation of the structural integrity of AMPA-Rs.

### Effect of DDM treatment on the conformation of AMPA-Rs

Our previous study demonstrated that native AMPA-R complexes can adopt a variety of conformations (Nakagawa et al., 2005). Based on the relative position of the two NTD dimers, we classified particles into two classes. In type I particles, the two NTD dimers are close together and asymmetrically stacked on top of each other (Figure 2A, left panel). Type 2 particles are those in which the two NTD dimers are separated, giving the particles a V-shaped appearance with a pseudo two-fold symmetry (Figure 2A, right panel). In preparations of native AMPA-R complexes purified in CHAPS, a slightly greater number of particles adopted the type I conformation in the absence of any drugs (type I 60% and type II 40%), but almost all the particles adopted a type II conformation in the presence of glutamate (Nakagawa et al., 2005). From these results we concluded that the different conformational states are related to different functional states of the ligand-gated ion channel, and that the type II conformation is characteristic for AMPA-Rs in the desensitized state. When we analyzed the conformational distribution of AMPA-Rs in the absence of associated stargazin/TARP proteins, using the same approach described previously (Nakagawa et al., 2005), we found that in the absence of any drugs, the ratio of type I to type II particles was similar to that in the presence of stargazin/TARP proteins (type I 50% and type II 50%).

### Projection images of AMPA-Rs prepared by cryo-negative staining

In the type II conformation, the two NTD dimers radiate at varying angles from the transmembrane domain, suggesting that the NTDs are attached to the TMD by rather flexible linkers. Particles in the type I conformation have a more defined appearance, which is probably due to the stacking interactions of the two NTD dimers on top of the LBD. We therefore decided to calculate a 3D reconstruction using the more defined particles in the Type I conformation.

To determine the 3D structure of AMPA-R complexes in the absence of stargazin/TARP proteins, we prepared AMPA-Rs (isolated in CHAPS and then treated with DDM) by cryo-negative staining. This specimen preparation technique combines the high image contrast provided by negative staining with the prevention of drying artifacts due to sample vitrification. As shown in Figure 2B, AMPA-Rs prepared by cryo-negative staining were monodispersed and homogeneous in size, and they adsorbed to the carbon support film in preferred orientations. While this reduced the heterogeneity of the particles in the images, it also made it necessary to calculate a 3D reconstruction with the random conical tilt approach, which requires images of tilted specimens to

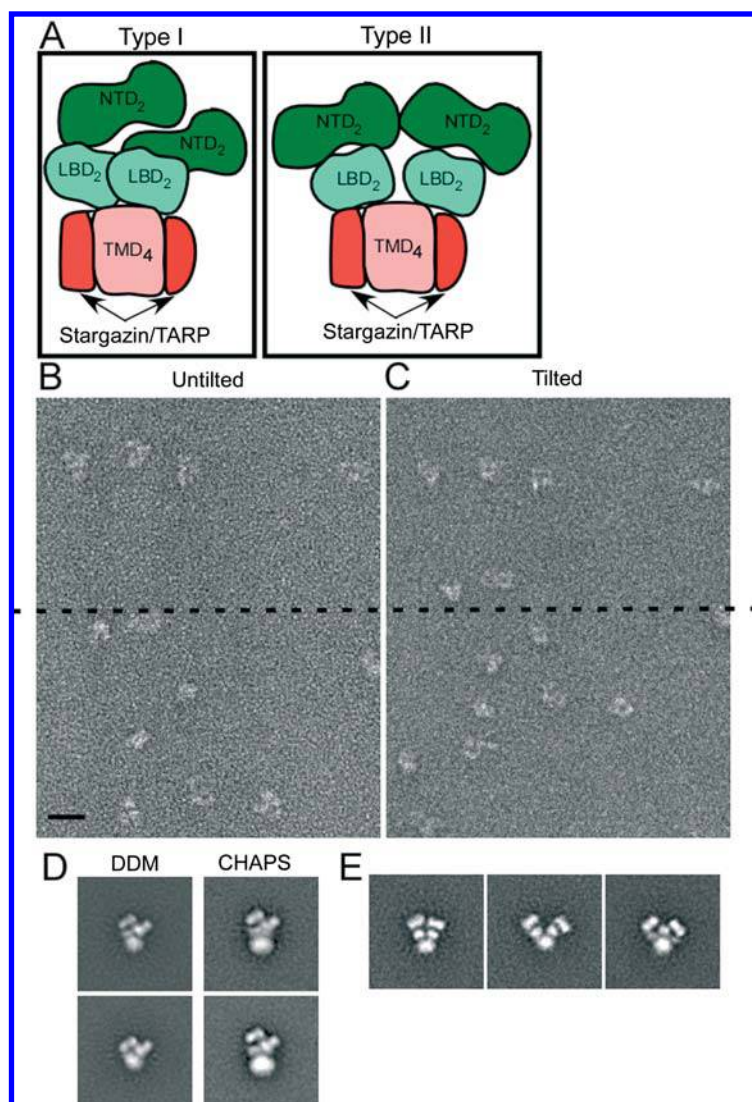


**Figure 2** Cryo-negative staining of AMPA-Rs in different conformations.

(A) Cartoon of AMPA-R complexes in type I (left panel) and type II conformations (right panel). (B) Image area of an untilted specimen of DDM-treated AMPA-Rs prepared by cryo-negative staining. Scale bar: 20 nm. (C) Same image area as in (B) of the specimen tilted to 50°. The broken line indicates the tilt axis. (D) Representative class averages of AMPA-Rs in type I conformation. The left column shows AMPA-Rs purified in CHAPS and treated with DDM. For comparison, the right column shows CHAPS-solubilized particles that were not treated with DDM. The difference in size of the transmembrane domain corresponds to the presence or absence of stargazin/TARP proteins. The size of each box is 50×50 nm. (E) Representative class averages of AMPA-Rs in Type II conformation. The class averages were obtained with AMPA-Rs purified in CHAPS and treated with DDM.

be collected. We therefore recorded a total of 109 image pairs at tilt angles of 0° and 50° (Figure 2B, C), from which we interactively selected 33 271 particle pairs using the display program WEB (Frank et al., 1996). After rejecting damaged or incompletely stain-embedded particles, the remaining 16 681 particles from the untilted images were subjected to 10 cycles of multivariate statistical analysis, multi-reference alignment and classification into 100 classes.

Representative class averages of the cryo-negatively stained AMPA-Rs that were treated with DDM are shown in Figure 2D, E. Figure 2D shows examples of particles in type I conformation and Figure 2E examples of those in type II conformation. For comparison, Figure 2D also shows class averages of native type I AMPA-R complexes that were prepared in CHAPS and not treated with DDM. As with our previous results using a conventional

negative staining procedure (Nakagawa et al., 2005), the density representing the transmembrane domain was significantly smaller in class averages of DDM-treated AMPA-R particles than in those of untreated particles, consistent with the removal of the stargazin/TARP proteins by treatment with DDM.

### 3D reconstruction of an AMPA-R without associated stargazin/TARP proteins

To calculate a 3D reconstruction, we combined the two classes of particles in type I conformation (572 particles) that showed the finest structure and used these particle images to calculate a 3D density map using the random conical tilt approach (Frank, 1996) implemented in SPIDER (Frank et al., 1996). The resulting density map was used as a reference model for further refinement of the

orientational parameters of the particles with FREALIGN (Stewart and Grigorieff, 2004), which was also used for correction of the contrast transfer function. To assess the consistency of the final 3D reconstruction (Figure 3A) with the raw data, particle images were compared with corresponding reprojections from the reconstructed 3D density map, showing that the reprojections were in good agreement with the particle images (Figure 3B). The Euler angles assigned to the particles were also consistent with the distribution expected for a random conical tilt reconstruction (Figure 3C). Based on Fourier shell correlation (FSC), the resolution of the final density map was estimated to be 33 Å with the FSC=0.124 criterion (Rosenthal and Henderson, 2003) and 45 Å with the more conservative FSC=0.5 criterion.

The density representing the transmembrane domain in the final 3D map of the DDM-treated particles is significantly smaller than the densities representing the extracellular domains (Figure 3A). This differs from the density map we previously obtained for native AMPA-R complexes with the associated stargazin/TARP proteins, in which the width of the transmembrane domain was comparable to that of the extracellular domains (Naka-

gawa et al., 2005). The asymmetry of the molecule is still most prominent in the region of the NTDs, as it was in the structure of the type I AMPA-R complex with stargazin/TARP proteins (Nakagawa et al., 2005). There is a subtle difference in the arrangement of the NTDs in the AMPA-Rs with and without associated stargazin/TARP proteins, as the asymmetry observed at the level of the NTDs was slightly more pronounced when stargazin/TARP proteins were present. This may be related to the recently described differences in desensitization kinetics of AMPA-Rs in the presence or absence of associated stargazin/TARP proteins (Yamazaki et al., 2004; Priel et al., 2005; Tomita et al., 2005). It is equally likely, however, that the difference in the arrangement of the NTDs is simply caused by different deformations induced by the negative staining procedure.

### Interpretation of the AMPA-R structure

As before, we used crystal structures to interpret our 3D reconstruction of the AMPA-R. The LBD of GluR2 (Armstrong and Gouaux, 2000; Sun et al., 2002) is the only crystal structure available for an AMPA-R domain. How-

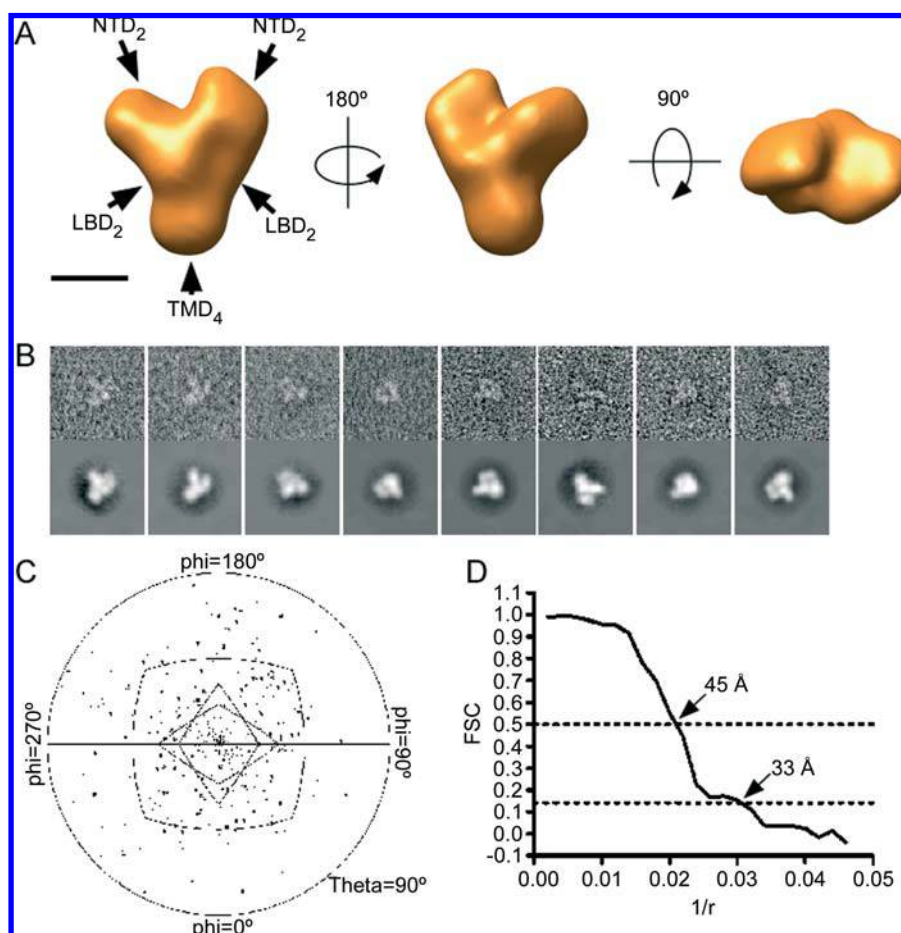


**Figure 3** 3D reconstruction of an AMPA-R without associated stargazin/TARP proteins.

(A) Views of the surface-rendered random conical tilt reconstruction of an AMPA-R without associated stargazin/TARP proteins. Note the overall asymmetry of the hetero-tetramer and the small transmembrane domain. NTD<sub>2</sub>, NTD dimer; LBD<sub>2</sub>, LBD dimer; TMD<sub>4</sub>, tetrameric TMD. Scale bar: 6.25 nm. (B) Comparison of raw particle images (upper panels) with corresponding reprojections from the 3D reconstruction (lower panels). The side length of the individual panels is 40 nm. (C) Plot of the Euler angles assigned to the individual particle images. The distribution of the angles is consistent with that expected for a random conical tilt reconstruction using images of specimens tilted to 0° and 50°. (D) The Fourier shell correlation (FSC) curve suggests a resolution of 33 Å with the FSC=0.124 criterion (Rosenthal and Henderson, 2003) or of 45 Å with the FSC=0.5 criterion.

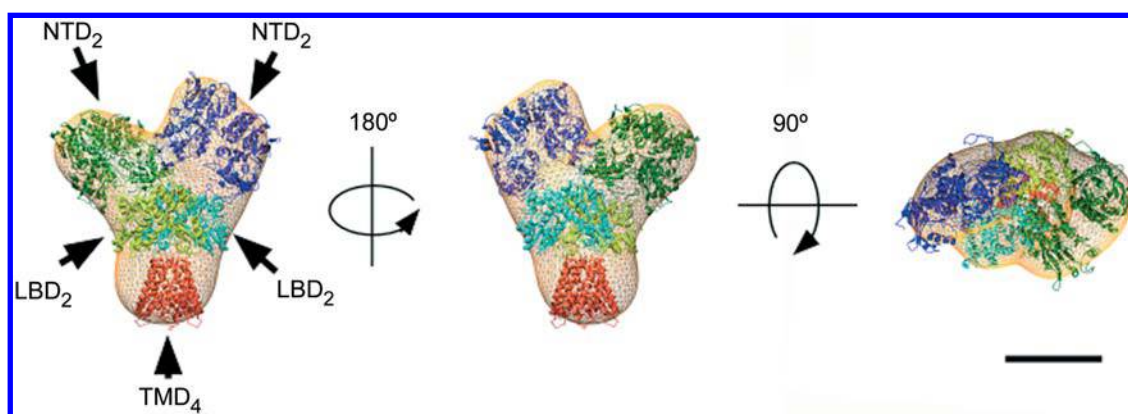


**Figure 4** Placement of the known crystal structures into the EM density map.

The crystal structures used are the extracellular domain of mGluR1 (PDB: 1EWV; dark blue and dark green) for the NTD, the ligand-binding domain of GluR2 (PDB: 1LBC; light blue and light green) for the LBD, and the transmembrane segment of KcsA (PDB: 1BL8; red) for the TMD. Scale bar: 6.25 nm.

ever, the NTDs of the AMPA-R subunits show high homology to both the bacterial periplasmic amino acid-binding protein LIVBP (Nakanishi et al., 1990) and the extracellular domain of metabotropic glutamate receptors (mGluRs). Interestingly, the extracellular domain of mGluR1 (Kunishima et al., 2000), as well as the LBD of GluR2, crystallize as dimers (Armstrong and Gouaux, 2000; Sun et al., 2002). Consistent with the proposed dimer-of-dimers organization of AMPA-Rs, the volume of the extracellular domain in our density map nicely accommodated two dimeric crystal structures, each of the mGluR1 extracellular domain and the GluR2 LBD (Figure 4).

The M1–M3 membrane segments of AMPA-R subunits are related to the prokaryotic KcsA potassium channel (Doyle et al., 1998), but the helices in AMPA-Rs and KcsA are inserted into the membrane in opposite orientations. In addition, AMPA-Rs have an additional M4 transmembrane segment that is absent from the KcsA channel. Placing the KcsA channel core into the density representing the transmembrane domain of the AMPA-R accounts for most of the density in the 3D reconstruction (Figure 4). The remaining unoccupied density can be explained by the additional M4 transmembrane segments of the four AMPA-R subunits in the heterotetramer.

Because of the limited resolution of our EM map, we did not refine the position of the crystal structures using computational algorithms. However, placement of the crystal structures into our 3D reconstruction demonstrates that the size and shape of the densities representing the individual domains of the AMPA-R subunits are compatible with the known crystal structures. Our results thus show that most of the mass of the tetrameric AMPA-R is located on the extracellular side, while stargazin/TARP proteins associate with the AMPA-R around the transmembrane region.

## Discussion

The proposed membrane topology of AMPA-R subunits predicts that, if native AMPA-R complexes consisted

exclusively of four AMPA-R subunits, the majority of the mass should be located on the extracellular side of the membrane. In contrast to this prediction, the transmembrane domain in our single particle reconstruction of native AMPA-R complexes was represented by a substantial density (Nakagawa et al., 2005). Furthermore, attempts to model the transmembrane domain of native AMPA-R complexes with the crystal structure of the KcsA potassium channel (Doyle et al., 1998) made it clear that the density in the EM map was too large to only represent the transmembrane domain of a heterotetrameric AMPA-R. The unoccupied density was also too large to be explained by the four additional M4 transmembrane segments that are found in AMPA-R subunits but absent from the KcsA channel.

We first suspected that the additional density was due to tightly bound lipids, but a silver staining method that we routinely use to detect co-purifying lipids showed that our AMPA-R preparation was free of phospholipids. Moreover, treatment with phospholipase A2 had no effect on the appearance of the particles and in particular the size of the transmembrane domain was unchanged (data not shown). SDS PAGE of a concentrated AMPA-R sample finally revealed two additional bands of clusters of small-molecular-weight proteins that co-purified with the AMPA-Rs. Identification of these bands by mass spectrometry revealed that they contained members of the stargazin/TARP family. Therefore, ligand-gated ion channels formed by AMPA-R subunits associate with additional membrane proteins of the stargazin/TARP family, a finding that has recently also been reported by another group (Fukata et al., 2005; Vandenberghe et al., 2005b).

Of the detergents we tested, native AMPA-R complexes composed of AMPA-R subunits and stargazin/TARP proteins were only stable in CHAPS. DDM, DM and OG destabilized the association of the stargazin/TARP proteins with the AMPA-R subunits. In this small test series, the harsher the detergent, i.e., the shorter the hydrophobic acyl chain and the smaller the hydrophilic head group, the more stargazin/TARP proteins were removed from the complex. However, the harsher detergents also began to destabilize the AMPA-R tetramers and in OG almost all AMPA-Rs dissociated into individual subunits.

It is difficult to speculate why CHAPS but not DDM maintains the association of stargazin/TARP proteins with AMPA-Rs, but the interaction between AMPA-R subunits and stargazin/TARP proteins appears to be hydrophobic in nature, as it is sensitive to the detergent used to keep the complex in solution.

It remains to be determined whether all AMPA-Rs in the brain are associated with proteins of the stargazin/TARP family. It is well established, however, that in the cerebellum the interaction of AMPA-Rs with stargazin/TARP proteins plays a critical role in synaptic targeting of the complex (Chen et al., 2000). The association of the four AMPA-R subunits (GluR1–4) with the four members of the stargazin/TARP family ( $\gamma$ -2,  $\gamma$ -3,  $\gamma$ -4, and  $\gamma$ -8) predicts a large variability in the molecular composition of native AMPA-R complexes. Whether different members of the stargazin/TARP family have a different effect on the activity of AMPA-Rs is unknown, but such variability in subunit composition is likely to amplify the molecular heterogeneity of AMPA-R complexes in different synapses. Thus, identifying the precise stoichiometry and molecular composition of AMPA-R complexes in the brain is now a priority. Interestingly, in *Caenorhabditis elegans* another membrane protein, SOL-1, is essential for the channel function of glutamate receptors, and it co-immunoprecipitates with glutamate receptors (Zheng et al., 2004). Furthermore, the NMDA subtype of glutamate receptors has been shown to immunoprecipitate with the Eph receptors at the synapses, which also affect the channel function (Dalva et al., 2000; Takasu et al., 2002). Taking these findings together, it seems likely that the interaction with other membrane proteins is an important characteristic of a subset of the glutamate receptor family of ligand-gated ion channel. Modulation of glutamate receptors in the synapse is believed to have a direct impact on information storage in the brain. In fact it has recently been shown that stargazin/TARP proteins can affect the desensitizing kinetics of AMPA-Rs (Yamazaki et al., 2004; Priel et al., 2005; Tomita et al., 2005). When administered, modulators of AMPA-Rs result in a change in cognition and alleviate neurological disease conditions (Staubli et al., 1994; Paul and Skolnick, 2003; Black, 2005). Thus, understanding the molecular and structural basis of the modulation of glutamate receptors by associating membrane proteins is likely to contribute to the design of modulator drugs that can act on these important receptor channels.

The single-particle EM reconstruction of the homo-tetramer formed by GluR2 that was expressed and purified from Sf9 insect cells looks significantly different from our structure (Tichelaar et al., 2004). The GluR2 homo-tetramer appears to have a true two-fold symmetry, whereas our purified hetero-tetrameric AMPA-R, in particular in the type I conformation, shows no structural symmetry. The difference between the structures may be explained by the difference between a homo- and a hetero-tetramer. Alternatively, it is conceivable that stargazin/TARP proteins assist proper folding of the AMPA-R, which is in keeping with the proposed function of stargazin/TARP proteins, which supposes that their association is important for the surface delivery of AMPA-Rs. Stargazin/TARP interaction may thus be important for the AMPA-R to

pass through the quality control mechanism in the ER (Vandenberghe et al., 2005a). The majority of AMPA-Rs in the brain are thought to be hetero-tetrameric (Wenthold et al., 1996). Interestingly, the conductance of the channel assembled by homo-tetrameric GluR2 is reported to be significantly smaller than the hetero-tetrameric AMPA-Rs (Swanson et al., 1997). Furthermore, subunit specific functions of the GluRs are also implicated in the rules that govern the trafficking of the AMPA-R to the synapse (Malinow and Malenka, 2002). Because native AMPA-Rs are mainly heteromeric (Wenthold et al., 1996), our structure is more likely to reflect the *in vivo* state of the AMPA-Rs.

## Materials and methods

### Protein purification

Native AMPA-R complexes were purified as previously described (Nakagawa et al., 2005). Briefly, synaptosome-enriched membranes isolated from rat brains were solubilized with 1% CHAPS and further purified by immunoaffinity chromatography using immobilized anti-GluR2 antibody. Bound AMPA-Rs were eluted with a competitive peptide corresponding to the epitope of the antibody. Purity of the preparation was further improved by gel filtration chromatography on a Superdex 200 column (Amersham, Uppsala, Sweden). Unless otherwise specified, native AMPA-R complex refers to protein purified by this method. To remove stargazin/TARP proteins, native AMPA-R complexes were run through a gel filtration column in a buffer containing 0.3% DM, 0.1% DDM, or 1% OG.

### Specimen preparation and electron microscopy

Negative staining and cryo-negative staining with 0.75% (w/v) uranyl formate were performed as previously described (Ohi et al., 2004). Images were recorded using a Tecnai T12 electron microscope (FEI) equipped with an LaB<sub>6</sub> filament and operated at an acceleration voltage of 120 kV. For specimens prepared by conventional negative staining, images were taken at a magnification of 52 000 $\times$  using a defocus value of -1.5  $\mu$ m. Grids of cryo-negatively stained specimens, used to collect image pairs of specimens tilted to 50° and 0°, were loaded on an Oxford cryo-transfer holder and maintained at liquid nitrogen temperature during image acquisition. Images were taken at a magnification of 42 000 $\times$ , with a defocus value of -1.5  $\mu$ m for images of the untilted specimens and -1.8  $\mu$ m for those from specimens tilted to 50°. All images were recorded using low-dose procedures on Kodak SO-163 film and developed for 12 min with full-strength Kodak D-19 developer at 20°C.

### Image processing

Electron micrographs were digitized with a SCAI scanner (Zeiss, Oberkochen, Germany) using a step size of 7  $\mu$ m and 3 $\times$ 3 pixels were averaged to obtain a pixel size on the specimen level of 4.04 Å for negatively stained and 5 Å for cryo-negatively stained specimens. Image processing was performed with the SPIDER software package (Frank et al., 1996). Projection averages were calculated over 10 cycles of K-means classification and multi-reference alignment specifying 100 output classes.

For 3D reconstructions of the cryo-negatively stained preparations, particle pairs were interactively selected from a total of 373 image pairs using WEB, the display program associated with SPIDER, and windowed into small images of 100 $\times$ 100 pixels. Particles from the images of untilted specimens were

used for classification into 100 classes as before. Images of the tilted specimen in each class were used to calculate initial 3D reconstructions of individual classes by back-projection, back-projection refinement, and angular refinement. The final volume obtained by angular refinement with SPIDER was used as the input model for FREALIGN (Stewart and Grigorieff, 2004), which was used for further refinement of the orientational parameters of the individual particles and to correct each particle image for the contrast transfer function according to its defocus value. The defocus value for each particle image was deduced from the position of the particles in the images and the tilt angles and defocus values of the images, which were determined with CTFTILT (Mindell and Grigorieff, 2003). Electron micrographs showing a high degree of astigmatism were discarded. Particles selected from images of both tilted and untilted specimens were used for FREALIGN refinement. The resolution of the final 3D reconstruction was estimated by Fourier shell correlation (FSC) and was 45 Å using the FSC=0.5 criterion and 33 Å using the FSC=0.142 criterion (Rosenthal and Henderson, 2003).

The crystal structures used to represent individual domains of AMPA-R subunits were the extracellular domain of mGluR1 (PDB: 1EWW) for the NTD, the ligand-binding domain of GluR2 (PDB: 1LBC) for the LBD, and the KcsA potassium channel (PDB: 1BL8) for the TMD. These crystal structures were manually docked into the EM density map using Chimera (Pettersen et al., 2004). Due to the limited resolution of the 3D reconstruction, no attempts were made to refine the docking of the crystal structures into the density map using computational algorithms.

## Acknowledgments

The molecular EM facility at Harvard Medical School was established with a generous donation from the Giovanni Armenise Harvard Center for Structural Biology. This work was supported by NIH grant GM62580 (to T.W.), which also provides funds to maintain the EM facility. M.S. is an investigator of the Howard Hughes Medical Institute.

## References

- Armstrong, N. and Gouaux, E. (2000). Mechanisms for activation and antagonism of an AMPA-sensitive glutamate receptor: crystal structures of the GluR2 ligand binding core. *Neuron* 28, 165–181.
- Black, M.D. (2005). Therapeutic potential of positive AMPA modulators and their relationship to AMPA receptor subunits. A review of preclinical data. *Psychopharmacology (Berl.)* 179, 154–163.
- Chen, L., Chetkovich, D.M., Petralia, R.S., Sweeney, N.T., Kawasaki, Y., Wenthold, R.J., Brecht, D.S., and Nicoll, R.A. (2000). Stargazin regulates synaptic targeting of AMPA receptors by two distinct mechanisms. *Nature* 408, 936–943.
- Dalva, M.B., Takasu, M.A., Lin, M.Z., Shamah, S.M., Hu, L., Gale, N.W., and Greenberg, M.E. (2000). EphB receptors interact with NMDA receptors and regulate excitatory synapse formation. *Cell* 103, 945–956.
- Dingledine, R., Borges, K., Bowie, D., and Traynelis, S.F. (1999). The glutamate receptor ion channels. *Pharmacol. Rev.* 51, 7–61.
- Doyle, D.A., Morais Cabral, J., Pfuetzner, R.A., Kuo, A., Gulbis, J.M., Cohen, S.L., Chait, B.T., and MacKinnon, R. (1998). The structure of the potassium channel: molecular basis of K<sup>+</sup> conduction and selectivity. *Science* 280, 69–77.
- Frank, J. (1996). *Three-Dimensional Electron Microscopy of Macromolecular Assemblies* (San Diego, USA: Academic Press).
- Frank, J., Radermacher, M., Penczek, P., Zhu, J., Li, Y., Ladjadj, M., and Leith, A. (1996). SPIDER and WEB: processing and visualization of images in 3D electron microscopy and related fields. *J. Struct. Biol.* 116, 190–199.
- Fukata, Y., Tzingounis, A.V., Trinidad, J.C., Fukata, M., Burlingame, A.L., Nicoll, R.A., and Brecht, D.S. (2005). Molecular constituents of neuronal AMPA receptors. *J. Cell Biol.* 169, 399–404.
- Gouaux, E. (2004). Structure and function of AMPA receptors. *J. Physiol.* 554, 249–253.
- Hollmann, M., O'Shea-Greenfield, A., Rogers, S.W., and Heinemann, S. (1989). Cloning by functional expression of a member of the glutamate receptor family. *Nature* 342, 643–648.
- Keinanen, K., Wisden, W., Sommer, B., Werner, P., Herb, A., Verdoorn, T.A., Sakmann, B., and Seeburg, P.H. (1990). A family of AMPA-selective glutamate receptors. *Science* 249, 556–560.
- Kunishima, N., Shimada, Y., Tsuji, Y., Sato, T., Yamamoto, M., Kumasaka, T., Nakanishi, S., Jingami, H., and Morikawa, K. (2000). Structural basis of glutamate recognition by a dimeric metabotropic glutamate receptor. *Nature* 407, 971–977.
- Letts, V.A., Felix, R., Biddlecome, G.H., Arikath, J., Mahaffey, C.L., Valenzuela, A., Bartlett, F.S. II, Mori, Y., Campbell, K.P., and Frankel, W.N. (1998). The mouse stargazer gene encodes a neuronal Ca<sup>2+</sup>-channel gamma subunit. *Nat. Genet.* 19, 340–347.
- Malinow, R. and Malenka, R.C. (2002). AMPA receptor trafficking and synaptic plasticity. *Annu. Rev. Neurosci.* 25, 103–126.
- Mindell, J.A. and Grigorieff, N. (2003). Accurate determination of local defocus and specimen tilt in electron microscopy. *J. Struct. Biol.* 142, 334–347.
- Nakagawa, T., Cheng, Y., Ramm, E., Sheng, M., and Walz, T. (2005). Structure and different conformational states of native AMPA receptor complexes. *Nature* 433, 545–549.
- Nakanishi, N., Shneider, N.A., and Axel, R. (1990). A family of glutamate receptor genes: evidence for the formation of heteromultimeric receptors with distinct channel properties. *Neuron* 5, 569–581.
- Ohi, M., Li, Y., Cheng, Y., and Walz, T. (2004). Negative staining and image classification – powerful tools in modern electron microscopy. *Biol. Proced. Online* 6, 23–34.
- Paul, I.A. and Skolnick, P. (2003). Glutamate and depression: clinical and preclinical studies. *Ann. N.Y. Acad. Sci.* 1003, 250–272.
- Pettersen, E.F., Goddard, T.D., Huang, C.C., Couch, G.S., Greenblatt, D.M., Meng, E.C., and Ferrin, T.E. (2004). UCSF Chimera – a visualization system for exploratory research and analysis. *J. Comput. Chem.* 25, 1605–1612.
- Priel, A., Kollerker, A., Ayalon, G., Gillor, M., Osten, P., and Stern-Bach, Y. (2005). Stargazin reduces desensitization and slows deactivation of the AMPA-type glutamate receptors. *J. Neurosci.* 25, 2682–2686.
- Rosenmund, C., Stern-Bach, Y., and Stevens, C.F. (1998). The tetrameric structure of a glutamate receptor channel. *Science* 280, 1596–1599.
- Rosenthal, P.B. and Henderson, R. (2003). Optimal determination of particle orientation, absolute hand, and contrast loss in single-particle electron cryomicroscopy. *J. Mol. Biol.* 333, 721–745.
- Staubli, U., Rogers, G., and Lynch, G. (1994). Facilitation of glutamate receptors enhances memory. *Proc. Natl. Acad. Sci. USA* 91, 777–781.
- Stewart, A. and Grigorieff, N. (2004). Noise bias in the refinement of structures derived from single particles. *Ultramicroscopy* 102, 67–84.
- Sun, Y., Olson, R., Horning, M., Armstrong, N., Mayer, M., and Gouaux, E. (2002). Mechanism of glutamate receptor desensitization. *Nature* 417, 245–253.
- Swanson, G.T., Kamboj, S.K., and Cull-Candy, S.G. (1997). Single-channel properties of recombinant AMPA receptors depend on RNA editing, splice variation, and subunit composition. *J. Neurosci.* 17, 58–69.

- Takasu, M.A., Dalva, M.B., Zigmond, R.E., and Greenberg, M.E. (2002). Modulation of NMDA receptor-dependent calcium influx and gene expression through EphB receptors. *Science* 295, 491–495.
- Tichelaar, W., Safferling, M., Keinanen, K., Stark, H., and Maden, D.R. (2004). The three-dimensional structure of an ionotropic glutamate receptor reveals a dimer-of-dimers assembly. *J. Mol. Biol.* 344, 435–442.
- Tomita, S., Chen, L., Kawasaki, Y., Petralia, R.S., Wenthold, R.J., Nicoll, R.A., and Brecht, D.S. (2003). Functional studies and distribution define a family of transmembrane AMPA receptor regulatory proteins. *J. Cell Biol.* 161, 805–816.
- Tomita, S., Adesnik, H., Sekiguchi, M., Zhang, W., Wada, K., Howe, J.R., Nicoll, R.A., and Brecht, D.S. (2005). Stargazin modulates AMPA receptor gating and trafficking by distinct domains. *Nature* 435, 1052–1058.
- Vandenberghe, W., Nicoll, R.A., and Brecht, D.S. (2005a). Interaction with the unfolded protein response reveals a role for stargazin in biosynthetic AMPA receptor transport. *J. Neurosci.* 25, 1095–1102.
- Vandenberghe, W., Nicoll, R.A., and Brecht, D.S. (2005b). Stargazin is an AMPA receptor auxiliary subunit. *Proc. Natl. Acad. Sci. USA* 102, 485–490.
- Wenthold, R.J., Petralia, R.S., Blahos, J. II, and Niedzielski, A.S. (1996). Evidence for multiple AMPA receptor complexes in hippocampal CA1/CA2 neurons. *J. Neurosci.* 16, 1982–1989.
- Yamazaki, M., Ohno-Shosaku, T., Fukaya, M., Kano, M., Watanabe, M., and Sakimura, K. (2004). A novel action of stargazin as an enhancer of AMPA receptor activity. *Neurosci. Res.* 50, 369–374.
- Zheng, Y., Mellem, J.E., Brockie, P.J., Madsen, D.M., and Maricq, A.V. (2004). SOL-1 is a CUB-domain protein required for GLR-1 glutamate receptor function in *C. elegans*. *Nature* 427, 451–457.

Received July 21, 2005; accepted September 14, 2005